Published in final edited form as:
Cancer Res. 2010 April 1; 70(7): 2932–2941. doi:10.1158/0008-5472.CAN-09-3570.

Cyr61 mediates HGF-dependent tumor cell growth, migration and Akt activation

Courtney R. Goodwin[1,3], **Bachchu Lal**[1,2], **Xin Zhou**[1], **Sandra Ho**[1], **Shuli Xia**[1], **Alexandra Taeger**[1], **Jamie Murray**[1], and **John Laterra**[1,2,3,4]

[1]The Kennedy Krieger Institute, Johns Hopkins School of Medicine, Baltimore, MD.

[2]Department of Neurology, Johns Hopkins School of Medicine, Baltimore, MD.

[3]Department of Neuroscience, Johns Hopkins School of Medicine, Baltimore, MD.

[4]Department of Oncology, Johns Hopkins School of Medicine, Baltimore, MD.

Abstract

Certain tumor cell responses to the growth-factor inducible early response gene product CCN1/Cyr61 overlap with those induced by the HGF:c-Met signaling pathway. In this study, we investigate if Cyr61 is a downstream effector of HGF/c-Met pathway activation in human glioma cells. A semi-quantitative immunohistochemical analysis of 112 human glioma and normal brain specimens showed that levels of tumor-associated Cyr61 protein correlate with tumor grade ($P< 0.001$) and with c-Met protein expression ($R^2=0.4791$, $P<0.0001$). Purified HGF rapidly up-regulated Cyr61 mRNA (peak at 30 min) and protein expression (peak at 2 hr) in HGF-/c-Met$^+$ human glioma cell lines via a transcription- and translation-dependent mechanism. Conversely, HGF/c-Met pathway inhibitors reduced Cyr61 expression in HGF$^+$/c-Met$^+$ human glioma cell lines in vitro and in HGF$^+$/c-Met$^+$ glioma xenografts. Targeting Cyr61 expression with siRNA inhibited HGF-induced cell migration ($P < 0.01$) and cell growth ($P < 0.001$) in vitro. The effect of Cyr61 on HGF-induced Akt pathway activation was also examined. Cyr61 siRNA had no effect on the early phase of HGF-induced Akt activation (phospho-Ser-473) 30 min post-stimulation with HGF. Cyr61 siRNA inhibited a second phase of Akt phosphorylation measured 12 hr after cell stimulation with HGF and also inhibited HGF-induced phosphorylation of the Akt target GSK3α. We treated pre-established subcutaneous glioma xenografts with Cyr61 siRNA or control siRNA by direct intratumoral delivery. Cyr61 siRNA inhibited Cyr61 expression and glioma xenograft growth by up to 40% in a dose-dependent manner ($P < 0.05$). These results identify a Cyr61-dependent pathway by which c-Met activation mediates cell growth, cell migration, and long-lasting signaling events in glioma cell lines and possibly astroglial malignancies.

Keywords

Hepatocyte growth factor; c-Met; Cyr61; glioma siRNA; Akt; survival; migration

Introduction

Aberrations in receptor tyrosine kinase systems activate a multitude of oncogenic mechanisms that increase overall malignancy. The receptor tyrosine kinase c-Met and its multifunctional ligand hepatocyte growth factor (HGF) are overexpressed or hyperactivated in many solid

Corresponding Author: John Laterra, MD, PhD, The Kennedy Krieger Research Institute, 707 N. Broadway, Baltimore, MD 21205, Tel: 443-923-2679, Fax: 443-923-2695, Laterra@kennedykrieger.org .

neoplasms and correlate with poor patient survival in select malignancies. HGF/c-Met pathway activation can induce a variety of cell-type and context-dependent biological responses such as migration/invasion, proliferation, angiogenesis and cytoprotection (1–5). Inhibiting HGF and/or c-Met expression or function potently inhibits tumor xenograft formation, growth rates, and angiogenesis in many cancer model systems (6–9). The link between c-Met and malignant progression has stimulated the search for downstream mediators of these responses, in hope of understanding c-Met signaling and identifying new potential therapeutic targets.

c-Met is a potent activator of multiple signaling pathways, such as PI3K/Akt, Ras/MAPK, STAT, and NFκB which activate a wide variety of oncogenic targets (10,11). Expression microarray analysis of human glioblastoma cells stimulated with HGF resulted in the identification of several genes that are upregulated by c-Met activation. One HGF-responsive gene identified is the *C*ysteine-rich 61/*C*onnective tissue growth factor/*N*ephroblastoma overexpressed (CCN) family member Cyr61 (12). Cyr61 is a secreted heparin-binding protein that associates with the cell surface and extracellular matrix (13–15). Cyr61, which is normally involved in wound healing, chondrogenesis, and neovascularization in vivo, is a growth factor- and hypoxia-inducible early response gene that interacts with various cellular integrins to induce the expression of a diverse array of genes (14–18). Purified Cyr61 protein has been shown to regulate cell adhesion, stimulate chemotaxis, augment growth factor-induced DNA synthesis, foster cell survival, and enhance angiogenesis *in vivo* (19,20). Cyr61 expression has been linked to poor outcomes in a multitude of solid tumors (21,22), is implicated in increased tumorigenicity, and is overexpressed in invasive breast cancer and astrocytoma cell lines (23–28). Moreover, forced expression of Cyr61 in a low grade U343 glioma model markedly enhanced tumorigenicity and vascularization *in vivo*. Xie et al. demonstrated that multiple integrins, especially αvβ3, were upregulated by Cyr61 protein along with an increase in integrin linked kinase activity and AKT activation (20).

The overlapping phenotypic effects of c-Met activation and Cyr61 suggest a novel mechanism by which the HGF/c-Met pathway influences cell behavior. This paper investigates whether the HGF/c-Met pathway and Cyr61 are correlated in human gliomas and whether HGF induces Cyr61 in glioma models. Furthermore, we investigate if inhibiting Cyr61 in HGF-dependent glioma models alters HGF-induced cell survival, migration, and Akt activation. Our findings show that Cyr61 induction contributes to HGF-dependent glioma cell Akt activation, migration, cell proliferation, and tumor xenograft growth.

Materials and Methods

Cell Culture and Reagents

U373MG, U87MG, and SNB-19 cell lines were originally obtained from American Type Culture Collection (ATCC). Serial routine testing in our laboratory shows that these cells have maintained their characteristic phenotypic and gene expression patterns. U87MG cells were grown in Minimum Essential Medium w/ Earle Salts and L-glutamine (MEM 1X; Mediatech Inc. Inc.) supplemented with 10% fetal bovine serum (FBS; Gemini Bioproducts Inc.), 2 mM Sodium Pyruvate (Mediatech Inc.), 0.1 mM MEM-Non-essential Amino Acids (Mediatech Inc.) and penicillin-streptomycin (Mediatech Inc.). U373MG and SNB-19 cells were grown in Dulbecco's Modified Essential Medium low glucose with L-glutamine and sodium pyruvate (DMEM; Mediatech Inc. Inc.) supplemented with 10% fetal bovine serum and penicillin-streptomycin as previously described (29). All cells were grown at 37°C in a humidified incubator with 5% CO_2.

Antibodies

Antibodies were obtained from the following sources and used at the indicated dilutions: Abcam (Cambridge, MA)- CCN1/Cyr61 (Rabbit, 1:1000); Cell Signaling Technology (Beverly, MA)- phospho-GSK3α/β Serine$^{9/21}$ (Rabbit, 1:1000), phospho-Akt-serine^{473} (Rabbit, 1:1000); Santa Cruz Biotechnology (Santa Cruz, CA)- Cyr61 (Rabbit, 1:1000), actin (Rabbit, C-11; 1:1,000); BD Sciences (San Jose, CA) Total Akt (Mouse, 1:500); LI-COR Biosciences (Lincoln, NE)- secondary antibodies labeled with spectrally distinct near-infrared dyes IRDye 800CW (goat anti-mouse, 1:15,000) and IRDye 680CW (goat anti-Rabbit, 1:20,000). Murine mAbs: Anti-HGF L2G7 and the isotype matched control 5G8 were obtained from Galaxy Biotech, LLC (Mountainview, CA) and used as indicated (30).

Tumor xenografts

Glioma xenografts were generated as previously described (29). Female 6- to 8-week-old mice (National Cancer Institute, Frederick, MD) were anesthetized by i.p. injection of ketamine (100 mg/kg) and xylazine (5 mg/kg). For subcutaneous xenografts, Nu/nu mice received 4×10^6 cells in 0.05 mL of plain media s.c. in the dorsal flank. When tumors reached –200 mm^3, the mice were randomly divided into groups ($n = 5$ per group) and received the indicated doses of either L2G7 or isotype matched control mAb (5G8) in 0.1 ml PBS i.p. as previously described (30). Tumor volumes were estimated by measuring two dimensions [length (a) and width (b)] and calculating volume as $V = ab^2 / 2$ (30,31). At the end of each experiment, tumors were excised, frozen in liquid nitrogen and protein was extracted for immunoblot analysis.

For intracranial xenografts, Scid/beige mice received 1×10^5 cells /2 μl by stereotaxic injection into the right caudate/putamen (29). L2G7 or 5G8 mAb was administered as above. Groups of mice ($n = 5$) were sacrificed by perfusion fixation at the indicated times and the brains removed for histologic studies. Vibratome/ microtome perfusion-fixed tumor xenograft sections were subjected to quantitative infrared immunofluorescence by simultaneously staining with primary antibodies specific for Cyr61 and GAPDH using methods described by Kearn et al. (32) (www.licor.com). Secondary antibodies labeled with two spectrally distinct near-infrared dyes (IRDye 800CW goat anti-mouse 1:10,000, IRDye 680CW goat anti-Rabbit 1:10,000; LI-COR Biosciences) were used to simultaneously detect and quantify Cyr61 relative to GAPDH. Computer-assisted signal quantification was performed using the Odyssey Infrared Imager from LI-COR Biosciences.

The Johns Hopkins University Institutional Animal Care and Use Committee approved all animal protocols used in this study.

Immunohistochemistry and immunofluorescence

Cryostat or paraffin-embedded sections were stained with anti-Cyr61, anti-total Met, or anti-Ki67 using previously described methods (29). Biotinylated-conjugated secondary antibodies followed by incubation with 3, 3'-diaminobenzidine peroxidase substrate were used to detect primary Abs. Sections were counterstained with Gill's hematoxylin solution. We analyzed 3–4 random fields per histological section and 2 sections per tumor to generate an average value per individual tumor. The percent area of antibody staining or proliferation indices were determined by computer-assisted quantification using ImageJ Software (rsb.info.nih.gov/ij/). The Rabbit IgG control values were determined in adjacent serial sections for each field and subtracted from the raw Cyr61 or Met expression value (as determined by computer assisted image analysis software) to generate the final expression levels. Values > 2 standard deviations above the normal human brain clinical specimens were used as the cutoff point for overexpression of Cyr61 or Met in gliomas (20,28).

Northern Blot Analysis

Total RNA was harvested from cells using Qiagen RNeasy kits according to manufacturer's recommendations. Ten micrograms of RNA per sample were denatured with deionized glyoxal, combined with RNA loading buffer, and subjected to electrophoresis in either duplicate or triplicate on a 1.0% agarose gel containing ethidium bromide for 2.5 h at 60 V. RNA was transferred to a nylon membrane (Nytran; Schleicher & Schuell Bioscience) overnight in 10× SSC (1.5 mol/L NaCl, 0.15 mol/L sodium citrate). The cDNA probe for Cyr61 was synthesized using oligonucleotide primers (Sense: 5'- GGUUUACUUACGCUGGAUGtt – 3' and Anti-sense: 5' CAUCCAGCGUAAGUAAACCtg- 3') designed from accession NM_001554. Reverse transcription–PCR was performed using U373MG RNA as a template, and PCR products were subcloned in TOPO PCR cloning vectors (Invitrogen, Inc.) and sequenced before use. Northern blot probes were generated for Cyr61 and 28S rRNA with [32P]dCTP (Amersham-Pharmacia) using a random priming labeling kit (Roche Diagnostics) according to manufacturer's specifications. Membranes were prehybridized for 4 h at 42°C and then hybridized overnight at 42°C in a rotating oven. Membranes were washed thrice in 1X SSC 0.1% SDS at 50°C. Radioactivity was quantified using the Bio-Imaging analyzer BAS 2500 (Fuji Medical Systems). All blots were stripped and then rehybridized with cDNA probe specific for 28S rRNA. Data from western blots consist of control and experimental lanes quantified from the same membrane. Results are expressed relative to 28S rRNA. Each figure derived from these methods represents data from a single blot and single exposure condition. For a subset of experiments, representative lanes (shown below quantitative data) that most closely approximate the mean quantitative values were selected and repositioned from the original single blots to eliminate replicate lanes.

Cyr61 siRNAs

Predesigned siRNA's for Cyr61 were obtained from Ambion, Inc and Dharmacon. Three siRNA's (ID 144771, ID 144772, and ID10013; NM_001554) were screened for knockdown efficiency by Northern and Western blotting as described above. siRNA ID 144771 and Dharmacon's Cyr61 siRNA On TARGET Plus Human SMARTpool were used for experimental studies. U373 cells were plated in 10cm diameter tissue culture dishes at 5×10^5 cells per plate in high serum media (10% FBS). The next day, the medium was replaced with low serum medium (0.1% FBS). siRNAs were prepared using siPort Lipid (Ambion, Inc.) for in vitro studies as instructed by the manufacturer to obtain a final working siRNA concentration of 50 nmol/L. One hour after replacing the medium, siRNA complexes were added to cells and allowed to incubate for 48 h. For in vivo studies, siRNAs were prepared using *in vivo*-JET-PEI (Polyplus Transfection) as per manufacturer's instructions to obtain a final working treatment of 50–500 pmoles of Cyr61 siRNA in a total volume of 50uL.

Immunoblot analysis

Total protein was extracted from glioma xenografts and cells using radioimmunoprecipitation assay (RIPA) buffer (1% Igepal, 0.5% sodium deoxycholate, and 0.1% SDS in PBS) containing fresh 1X protease and 1X phosphatase inhibitors (Calbiochem) at 4°C. Tissue extracts were sonicated on ice and centrifuged at 5,000 RPM at 4°C for 5 minutes. Supernatants were assayed for protein concentrations by Coomassie protein assay (Pierce) according the manufacturer's recommendations. Aliquots of 40 or 60μg of total protein were combined with Laemmli loading buffer containing β-mercaptoethanol and subjected to SDS-polyacrylamide gel electrophoresis (PAGE) according to the method of Towbin et al. with some modifications (33,34). For immunoblot analyses, proteins were electrophoretically transferred to nitrocellulose membrane with a semidry transfer apparatus (GE Healthcare) at 50 mA for 60 minutes. Membranes were incubated for 1 h in Odyssey Licor Blocking Buffer at room temperature and then overnight with primary antibodies at 4°C in 5% BSA in Tris-buffered

saline (TBS) containing 0.1% Tween 20 (TBS/T). Membranes were then washed 3 X with TBS/T, incubated with secondary antibody at 1:10,000 for 1 h in TBS/T, washed 3 X with TBS/T, followed by washing 2 X with TBS. Proteins were detected and quantified using the Odyssey Infrared Imager (LI-COR Biosciences).

Cell Migration

U373MG cells were plated in 60mm gridded plates and treated with designated siRNAs. After 24 hours, cells were treated with mitomycin C (50μg/mL) for 2 hours and cells on each side of the grid lines were removed by scraping. Cells were placed in low serum (0.1% FBS) medium and stimulated with 50ng/mL HGF for 6 days. Cells were fixed and stained with Cresyl Violet. Computer-assisted image software was used to quantify cell migration relative to the grid line border.

Statistical methods

Statistical analysis consisted of one-way ANOVA followed by the Tukey or Dunnet's multiple-comparison-test using Prism (GraphPad software Inc., San Diego, CA). The χ^2 test and *t* test were used to analyze the association of Cyr61 (or Met) with each clinical characteristic (age, gender, pathology, and grade). $P < 0.05$ was considered significant. All experiments reported here represent at least three independent replications. Data are represented as mean values ± standard error of the mean (SEM).

Results

Cyr61 expression correlates with Met expression in human gliomas

Previous reports have shown that Cyr61 and Met expression both independently correlate with progression and malignancy in human gliomas (4,28,35). A correlation between Cyr61 and Met expression would support a potential mechanistic link between these proteins in glioma pathogenesis. We quantified the levels of Cyr61 and Met expression in 100 gliomas and 12 normal brain specimens by performing semi-quantitative immunohistochemistry on a paraffin-embedded human glioma tissue microarray (Biomax, Inc.) (Fig. 1). Met and Cyr61 were found to be overexpressed > 2 standard deviations higher (> 3-fold expression) than normal brain using criteria set forth by Xie et al. (28) in 35% and 41% of glioma samples, respectively. Over-expression of either Cyr61 or Met correlated with tumor grade ($P < 0.0001$) (Fig. 1A and 1B). We found that 27 out of 33 (82%) and 29 out of 33 (88%) WHO grade IV samples overexpressed Met and Cyr61, respectively. In comparison, 3 out of 25 (12%) and 3 out of 23 (13%) WHO grade III and II samples, respectively, overexpressed Met and 8 out of 25 (32%) and 3 out of 23 (13%) WHO grade III and II samples, respectively, overexpressed Cyr61. Using a 95 % confidence interval and regression analysis, we found that Cyr61 positively correlated with Met expression in human gliomas ($P < 0.0001$) (Fig. 1C).

Hepatocyte Growth Factor/ Scatter Factor-mediated expression of Cyr61 in glioma cell lines

Previous gene expression microarray analyses of U373 glioma cells treated with HGF identified Cyr61 as an HGF-inducible gene product (25). We hypothesized that HGF-induced glioma cell responses are mediated, in part, by Cyr61. To evaluate this hypothesis, we first defined the time course and magnitude of Cyr61 mRNA production and protein expression in response to HGF. Human U373 and SNB19 glioma cell lines were treated with HGF (50 ng/mL) for various time points, after which total cellular RNA, total cellular protein, and conditioned medium were isolated for Northern analysis or immunoblot analysis. Cyr61 mRNA expression was induced maximally 30–60 minutes after stimulation with HGF (Fig. 2A). Protein levels increased maximally 2–4 hours after HGF stimulation (Fig. 2B). Cyr61 protein accumulated in conditioned medium for up to 36 hrs after HGF stimulation (Fig. 2C).

HGF stimulation also induced Cyr61 in SNB19 (~50% increase) and U87 (~350% increase) cells (Suppl. Fig. 1A). We also examined U373 glioma cells engineered to stably express HGF (3) to determine if autocrine c-Met activation correlated with basal expression of Cyr61. The HGF-expressing clonal cell line had a ~2-fold higher expression of Cyr61, in comparison to wild type cells and HGF-negative transfected controls (Suppl. Fig. 1B). Both cycloheximide and actinomycin D potently inhibited HGF-induced Cyr61 expression, consistent with a transcriptional and translational mechanism of expression induction (Suppl. Fig. 1C).

Anti- HGF therapy inhibits Cyr61 protein expression concurrent with tumor growth inhibition in glioma xenograft models

We asked if Cyr61expression is altered by c-Met pathway inhibition in HGF/c-Met dependent glioma xenografts. Mice bearing pre-established c-Met^{+}/HGF^{+} subcutaneous glioma xenografts were treated with neutralizing anti-HGF mAbs (L2G7) or with isotype –matched control mAb (5G8) as previously reported (30). Anti-HGF therapy significantly inhibited the growth of both U87 tumor xenografts (Fig. 3A) and U373-SF55 xenografts (Fig. 3B). Anti-HGF therapy concurrently reduced xenograft Cyr61 expression by ~50% ($p < 0.05$) in U373-SF55 tumors and by ~25% in U87 tumors compared to controls. We also assessed the effect of anti-HGF mAbs on U87 intracranial tumor xenografts using quantitative dual wavelength near infrared integrative immunohistofluorescence imaging, which allows the simultaneous assessment of Cyr61 and GAPDH on tumor specific regions of interest in histologic sections (Fig. 3C). L2G7 significantly inhibited Cyr61 expression by ~20% ($P < 0.05$) in comparison to control mAb.

Cyr61 knockdown inhibits HGF-induced Akt signaling

HGF is a potent activator of the PI3K/Akt pathway and typically upregulates phospho-Akt maximally within 30 minutes of c-Met activation in c-Met expressing cells. Akt activation remains above non-stimulated levels as long as 24 hours post-HGF stimulation in glioma cell lines. We hypothesized that Cyr61-induction contributes to HGF-induced Akt activity at these later time points. Cyr61 small interfering RNA (siRNA) was used under conditions that achieved near-complete inhibition of HGF-induced Cyr61 expression as assessed by Western blot analysis (Fig. 4A and Suppl. Fig. 2A). We measured the time course of HGF-induced Akt phosphorylation (Ser473) in U373MG glioma cells treated with either control siRNA or Cyr61 siRNA. HGF induced a ~3-fold increase in Akt phosphorylation at 30 minutes in all treatment groups indicating that Cyr61 expression inhibition has no effect on the early phase of HGF-induced Akt phosphorylation. In contrast to that observed 30 min post-HGF stimulation, the induction of Akt phosphorylation at both 2 and 12 hours post-HGF stimulation was completely inhibited by Cyr61 siRNA (Fig. 4B). We examined the effect of Cyr61 expression knockdown on HGF-induced phosphorylation of the Akt target GSK-3α. At 24 hours post-HGF stimulation, phospho-GSK-3α (Ser21) was increased ~ 1.8-fold ($P < 0.05$) in control cells and in cells treated with scramble siRNA. Cyr61 siRNA inhibited HGF-induced phosphorylation of GSK-3α (Ser21) ($P < 0.05$) in comparison to scramble siRNA treated cells 24 hours post HGF-stimulation (Fig. 4C and Suppl. Fig. 2A).

Cyr61 knockdown inhibits HGF-induced glioma cell migration and proliferation

Since HGF induces Cyr61 expression, we hypothesized that Cyr61 expression contributes to the migration response of HGF-stimulated glioma cells. Cyr61 siRNAs significantly inhibited HGF-induced migration of growth arrested cells using a monolayer wound assay. Glioma cell migration was increased ~50% ($P < 0.01$) by HGF in control and scramble siRNA-treated cells (Fig. 5A). In contrast, HGF-induced migration was almost completely inhibited in Cyr61 siRNA-treated cells (Fig. 5A). U373 and U87 cells were treated with Cyr61 siRNAs +/− HGF and cell growth was quantified using MTT cell viability assays and cell death was quantified

by LDH release assay. Cyr61 siRNAs blunted HGF-induced cell proliferation by ~40% in U373 glioma cells (Fig. 5B). U87 glioma cells express both HGF and c-Met creating an autocrine loop for Met pathway activation. Cyr61 siRNAs also blunted cell proliferation by ~40–55% in U87 glioma cells consistent with the inhibition of an HGF-dependent autocrine pathway (Fig 5C). Cyr61 siRNA had no effect on LDH release under both basal and HGF-stimulated conditions (Suppl. Fig. 2B, C). Thus, Cyr61 contributes to HGF-dependent migration and cell proliferation, without influencing cell viability.

Targeting Cyr61 inhibits glioma growth in vivo

The in vitro findings led us to investigate whether Cyr61 expression knock-down decreases tumor xenograft growth in vivo. We examined the effect of transient Cyr61 siRNA treatment on the growth of HGF-dependent subcutaneous U87 tumor xenografts. U87 glioma cells were implanted in the flanks of nude mice and xenografts were allowed to grow to ~200mm^3. Control and Cyr61 siRNAs complexed to the JET-PEI in vivo transfection reagent were injected intratumorally once per day for 5 consecutive days. All mice were sacrificed 24 hours after the last intratumoral injection. Cyr61 siRNAs at a concentration of 500 pmoles statistically significantly inhibited both U87 glioma xenograft growth (Fig. 6A) and Cyr61 expression (Fig. 6B) by ~40% compared to animals treated with control siRNA ($P < 0.05$). The anti-tumor effects of Cyr61 siRNAs on U87 glioma xenograft growth could be explained, in part, by decreases in the cell proliferation response. Cyr61 siRNAs significantly inhibited tumor cell proliferation (i.e. Ki67 labeling) by ~57% compared to animals treated with control siRNA ($P < 0.001$) (Fig. 6C).

Discussion

Receptor tyrosine kinases have emerged as potent regulators of tumor malignancy. Understanding the multifaceted mechanisms of oncogenic RTK signaling will influence the application of currently approved therapies and potentially elucidate novel targets for future drug development. Here we show that the downstream effects of HGF/c-Met pathway activation are partly mediated through the Cyr61 oncogene. Specifically, we show that intratumoral Cyr61 levels correlate with the receptor tyrosine kinase Met in human tumors and that inhibiting this immediate early gene abrogates Akt dependent cell signaling and biological responses to hepatocyte growth factor/ c-Met activation. Specifically, Cyr61 siRNAs inhibited HGF-dependent glioma cell growth and migration in vitro and glioma xenograft growth in vivo. Our findings show that Cyr61 induction prolongs HGF-induced Akt-dependent signaling and its downstream biological effects. These results also suggest that glioma-associated Cyr61 protein levels can serve as a marker of HGF/c-Met pathway inhibition in HGF–dependent tumors.

Solid malignancies are commonly associated with multiple co-activated receptor pathways and the heterogeneous genetic backgrounds of these tumor subtypes warrant investigation into common RTK-regulated signaling molecules that may serve as therapeutic targets for drug development. Cyr61 has been implicated in tumor progression, exerting its effects by increasing cell proliferation, migration and angiogenesis (23–28). Furthermore, Cyr61 is known to be induced by a wide array of growth factors and signaling molecules involved in tumor malignancy, such as epidermal growth factor and platelet derived growth factor (24, 36). Recent evidence also suggests that Cyr61 transcription is mediated by activation of STAT3, a known RTK-initiated signaling cascade, suggesting a potential pathway by which RTK-mediated malignancies induce their effects (37). Induction of Cyr61 in these tumor models points to a potentially broader role for this oncogene in receptor tyrosine kinase regulated malignancies and suggests that Cyr61 could be a potential node of convergence for multiple RTK signaling pathways.

Hyperactivation of the PI3K/AKT pathway is strongly associated with tumor malignancy. Here we show that Cyr61 contributes to HGF induced activation of Akt and the phosphorylation of the Akt target GSK3. While not investigated in this study, this Akt response is likely to be mediated, at least in part, by focal adhesion kinase (FAK) and integrin linked kinase (ILK), intracellular tyrosine kinases involved in integrin-mediated signaling, cell migration, cell proliferation, and cell adhesion. Xie et al. has previously shown that forced expression of Cyr61 in low tumorigenic cell lines leads to increased ILK activity, AKT activation, and the malignant phenotype of glioma cells (20). Furthermore, RGD-peptide integrin inhibitors such as cilengitide and neutralizing antibody blockade of Cyr61's main binding partner, the integrin αvβ3, are shown to decrease ILK activity, AKT activation and cell proliferation in glioma and ovarian cancer cells (38,39). Previous studies found that siRNA directed to FAK and ILK inhibits AKT activation, however a direct link between Cyr61 and either FAK or ILK remains to be determined.

Our results reveal a novel pathway for HGF-induced Akt activation and suggest that the Cyr61-dependent prolongation of Akt activity is important in HGF induced cell responses. These studies help to elucidate the regulatory mechanisms underlying HGF/c-Met pathway activation, while also providing evidence supporting a mechanism of Akt activation that is RTK-induced via a non-classical pathway.

Supplementary Material

Refer to Web version on PubMed Central for supplementary material.

Acknowledgments

Financial Support: This work was supported by NIH grants NS32148 (JL), CA129192 (JL), the United Negro College Fund/Merck Science Initiative (CRG) and the American Federation for Aging Research (CRG).

References

1. Lamszus K, Laterra J, Westphal M, Rosen EM. Scatter factor/hepatocyte growth factor (SF/HGF) content and function in human gliomas. Int J Dev Neurosci 1999;17(5–6):517–530. [PubMed: 10571413]
2. Lamszus K, Schmidt NO, Jin L, et al. Scatter factor promotes motility of human glioma and neuromicrovascular endothelial cells. Int J Cancer 1998;75(1):19–28. [PubMed: 9426685]
3. Laterra J, Rosen E, Nam M, Ranganathan S, Fielding K, Johnston P. Scatter factor/hepatocyte growth factor expression enhances human glioblastoma tumorigenicity and growth. Biochem Biophys Res Commun 1997;235(3):743–747. [PubMed: 9207232]
4. Birchmeier C, Birchmeier W, Gherardi E, Vande Woude GF. Met, metastasis, motility and more. Nat Rev Mol Cell Biol 2003;4(12):915–925. [PubMed: 14685170]
5. Walter KA, Hossain MA, Luddy C, Goel N, Reznik TE, Laterra J. Scatter factor/hepatocyte growth factor stimulation of glioblastoma cell cycle progression through G(1) is c-Myc dependent and independent of p27 suppression, Cdk2 activation, or E2F1-dependent transcription. Mol Cell Biol 2002;22(8):2703–2715. [PubMed: 11909963]
6. Abounader R, Ranganathan S, Lal B, et al. Reversion of human glioblastoma malignancy by U1 small nuclear RNA/ribozyme targeting of scatter factor/hepatocyte growth factor and c-met expression. J Natl Cancer Inst 1999;91(18):1548–1556. [PubMed: 10491431]
7. Jin H, Yang R, Zheng Z, et al. MetMAb, the one-armed 5D5 anti-c-Met antibody, inhibits orthotopic pancreatic tumor growth and improves survival. Cancer Research 2008;68(11):4360–4368. [PubMed: 18519697]
8. Stabile LP, Rothstein ME, Keohavong P, et al. Therapeutic targeting of human hepatocyte growth factor with a single neutralizing monoclonal antibody reduces lung tumorigenesis. Molecular Cancer Therapeutics 2008;7(7):1913–1922. [PubMed: 18645002]

9. Du W, Hattori Y, Yamada T, et al. NK4, an antagonist of hepatocyte growth factor (HGF), inhibits growth of multiple myeloma cells: molecular targeting of angiogenic growth factor. Blood 2007;109 (7):3042–3049. [PubMed: 17179234]
10. Bellacosa A, Kumar CC, Di Cristofano A, Testa JR. Activation of AKT kinases in cancer: implications for therapeutic targeting. Adv Cancer Res 2005;94:29–86. [PubMed: 16095999]
11. Bowers DC, Fan S, Walter KA, et al. Scatter factor/hepatocyte growth factor protects against cytotoxic death in human glioblastoma via phosphatidylinositol 3-kinase-and AKT-dependent pathways. Cancer Research 2000;60(15):4277–4283. [PubMed: 10945642]
12. Abounader R, Reznik T, Colantuoni C, Martinez-Murillo F, Rosen EM, Laterra J. Regulation of c-Met-dependent gene expression by PTEN. Oncogene 2004;23(57):9173–9182. [PubMed: 15516982]
13. Chen N, Chen CC, Lau LF. Adhesion of human skin fibroblasts to Cyr61 is mediated through integrin alpha 6beta 1 and cell surface heparan sulfate proteoglycans. J Biol Chem 2000;275(32):24953–24961. [PubMed: 10821835]
14. Kireeva ML, Lam SC, Lau LF. Adhesion of human umbilical vein endothelial cells to the immediate-early gene product Cyr61 is mediated through integrin alphavbeta3. J Biol Chem 1998;273(5):3090–3096. [PubMed: 9446626]
15. Jedsadayanmata A, Chen CC, Kireeva ML, Lau LF, Lam SC. Activation-dependent adhesion of human platelets to Cyr61 and Fisp12/mouse connective tissue growth factor is mediated through integrin alpha(IIb)beta(3). J Biol Chem 1999;274(34):24321–24327. [PubMed: 10446209]
16. Meyuhas R, Pikarsky E, Tavor E, et al. A Key role for cyclic AMP-responsive element binding protein in hypoxia-mediated activation of the angiogenesis factor CCN1 (CYR61) in Tumor cells. Mol Cancer Res 2008;6(9):1397–1409. [PubMed: 18819928]
17. Babic AM, Kireeva ML, Kolesnikova TV, Lau LF. CYR61, a product of a growth factor-inducible immediate early gene, promotes angiogenesis and tumor growth. Proceedings of the National Academy of Sciences of the United States of America 1998;95(11):6355–6360. [PubMed: 9600969]
18. Wong M, Kireeva ML, Kolesnikova TV, Lau LF. Cyr61, product of a growth factor-inducible immediate-early gene, regulates chondrogenesis in mouse limb bud mesenchymal cells. Developmental Biology 1997;192(2):492–508. [PubMed: 9441684]
19. Menendez JA, Vellon L, Mehmi I, Teng PK, Griggs DW, Lupu R. A novel CYR61-triggered 'CYR61-alphavbeta3 integrin loop' regulates breast cancer cell survival and chemosensitivity through activation of ERK1/ERK2 MAPK signaling pathway. Oncogene 2005;24(5):761–779. [PubMed: 15592521]
20. Xie D, Yin D, Tong X, et al. Cyr61 is overexpressed in gliomas and involved in integrin-linked kinase-mediated Akt and beta-catenin-TCF/Lef signaling pathways. Cancer Research 2004;64(6):1987–1996. [PubMed: 15026334]
21. Mori A, Desmond JC, Komatsu N, et al. CYR61: a new measure of lung cancer outcome. Cancer Investigation 2007;25(8):738–741. [PubMed: 18058471]
22. O'Kelly J, Chung A, Lemp N, et al. Functional domains of CCN1 (Cyr61) regulate breast cancer progression. International Journal of Oncology 2008;33(1):59–67. [PubMed: 18575751]
23. Sakamoto S, Yokoyama M, Zhang X, et al. Increased expression of CYR61, an extracellular matrix signaling protein, in human benign prostatic hyperplasia and its regulation by lysophosphatidic acid. Endocrinology 2004;145(6):2929–2940. [PubMed: 14988385]
24. Sampath D, Winneker RC, Zhang Z. Cyr61, a member of the CCN family, is required for MCF-7 cell proliferation: regulation by 17beta-estradiol and overexpression in human breast cancer. Endocrinology 2001;142(6):2540–2548. [PubMed: 11356703]
25. Tsai MS, Hornby AE, Lakins J, Lupu R. Expression and function of CYR61, an angiogenic factor, in breast cancer cell lines and tumor biopsies. Cancer Research 2000;60(20):5603–5607. [PubMed: 11059746]
26. Xie D, Miller CW, O'Kelly J, et al. Breast cancer. Cyr61 is overexpressed, estrogen-inducible, and associated with more advanced disease. J Biol Chem 2001;276(17):14187–14194. [PubMed: 11297518]
27. Xie D, Nakachi K, Wang H, Elashoff R, Koeffler HP. Elevated levels of connective tissue growth factor, WISP-1, and CYR61 in primary breast cancers associated with more advanced features. Cancer Research 2001;61(24):8917–8923. [PubMed: 11751417]

28. Xie D, Yin D, Wang HJ, et al. Levels of expression of CYR61 and CTGF are prognostic for tumor progression and survival of individuals with gliomas. Clin Cancer Res 2004;10(6):2072–2081. [PubMed: 15041728]
29. Lal B, Xia S, Abounader R, Laterra J. Targeting the c-Met pathway potentiates glioblastoma responses to gamma-radiation. Clin Cancer Res 2005;11(12):4479–4486. [PubMed: 15958633]
30. Kim KJ, Wang L, Su YC, et al. Systemic anti-hepatocyte growth factor monoclonal antibody therapy induces the regression of intracranial glioma xenografts. Clin Cancer Res 2006;12(4):1292–1298. [PubMed: 16489086]
31. Tomayko MM, Reynolds CP. Determination of subcutaneous tumor size in athymic (nude) mice. Cancer Chemother Pharmacol 1989;24(3):148–154. [PubMed: 2544306]
32. Kearns EA, Simonson LG, Schutt RW, Johnson MJ, Neil LC. Characterization of monoclonal antibodies to two Treponema denticola serotypes by the indirect fluorescent-antibody assay. Microbios 1991;65(264–265):147–153. [PubMed: 2030646]
33. Reznik TE, Sang Y, Ma Y, et al. Transcription-dependent epidermal growth factor receptor activation by hepatocyte growth factor. Mol Cancer Res 2008;6(1):139–150. [PubMed: 18234969]
34. Towbin H, Staehelin T, Gordon J. Electrophoretic transfer of proteins from polyacrylamide gels to nitrocellulose sheets: procedure and some applications. Proceedings of the National Academy of Sciences of the United States of America 1979;76(9):4350–4354. [PubMed: 388439]
35. Koochekpour S, Jeffers M, Rulong S, et al. Met and hepatocyte growth factor/scatter factor expression in human gliomas. Cancer Research 1997;57(23):5391–5398. [PubMed: 9393765]
36. Liao HJ, de Los Santos J, Carpenter G. Contrasting role of phospholipase C-gamma1 in the expression of immediate early genes induced by epidermal or platelet-derived growth factors. Exp Cell Res 2006;312(6):807–816. [PubMed: 16427622]
37. Bourillot PY, Aksoy I, Schreiber V, et al. Novel STAT3 target genes exert distinct roles in the inhibition of mesoderm and endoderm differentiation in cooperation with Nanog. Stem cells (Dayton, Ohio) 2009;27(8):1760–1771.
38. Oliveira-Ferrer L, Hauschild J, Fiedler W, et al. Cilengitide induces cellular detachment and apoptosis in endothelial and glioma cells mediated by inhibition of FAK/src/AKT pathway. J Exp Clin Cancer Res 2008;27:86. [PubMed: 19114005]
39. Cruet-Hennequart S, Maubant S, Luis J, Gauduchon P, Staedel C, Dedhar S. alpha(v) integrins regulate cell proliferation through integrin-linked kinase (ILK) in ovarian cancer cells. Oncogene 2003;22(11):1688–1702. [PubMed: 12642872]

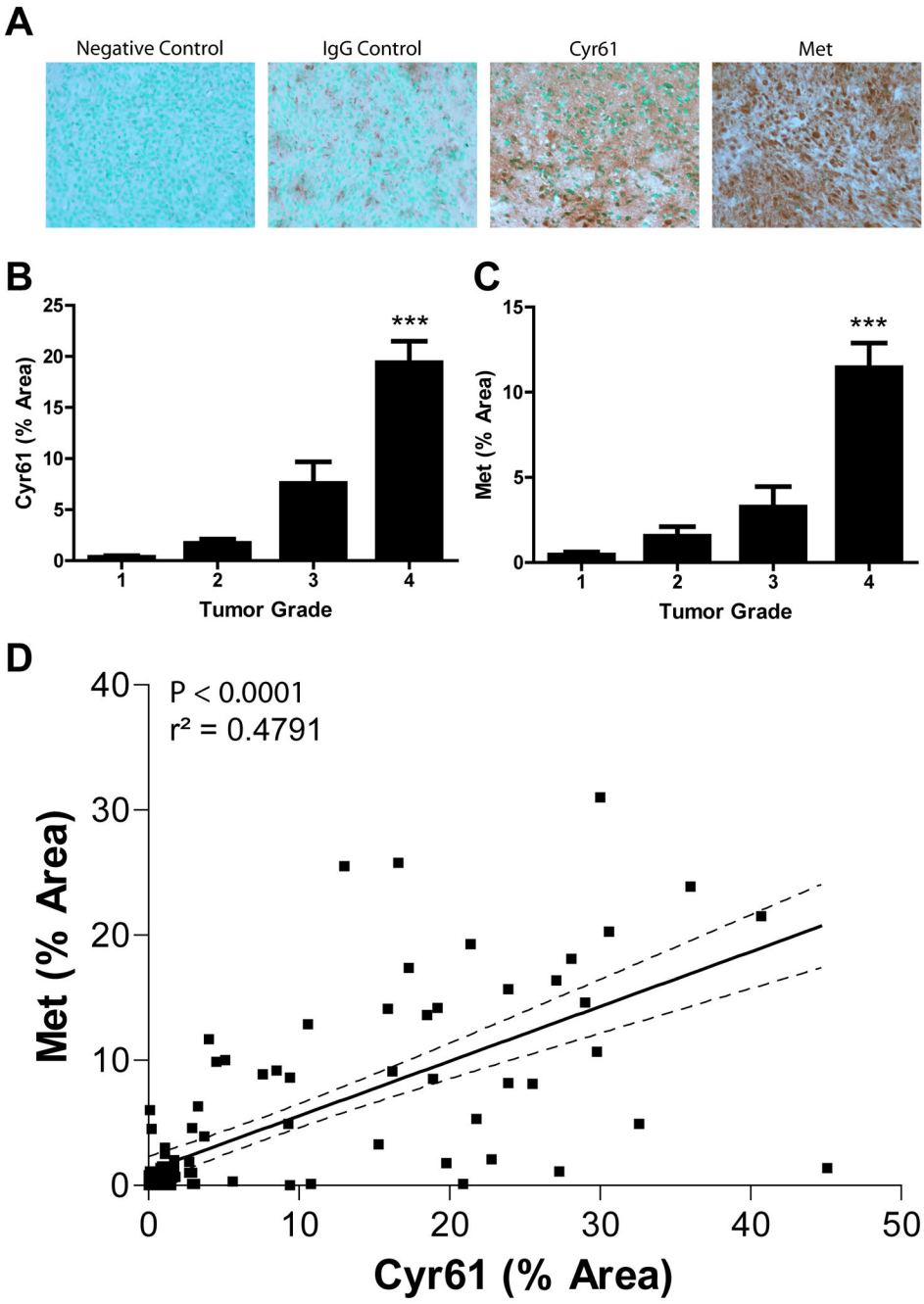

Figure 1. Met correlates with Cyr61expression in human gliomas

Semi-quantitative immunohistochemical staining of Met and Cyr61 in 100 human glioma samples (WHO Grade I-IV). A) Photomicrographs of immunohistochemically stained WHO Grade IV glioma sections showing negative control (unstained), and staining with non-immune IgG (IgG control), anti-Cyr61 (Cyr61) and anti-c-Met (Met). B) Average level of Met expression by tumor grade. C) Average level of Cyr61 expression by tumor grade. D) Linear regression analysis shows a positive correlation between Met and Cyr61 in human glioma tissues. *** $P < 0.001$ compared to controls.

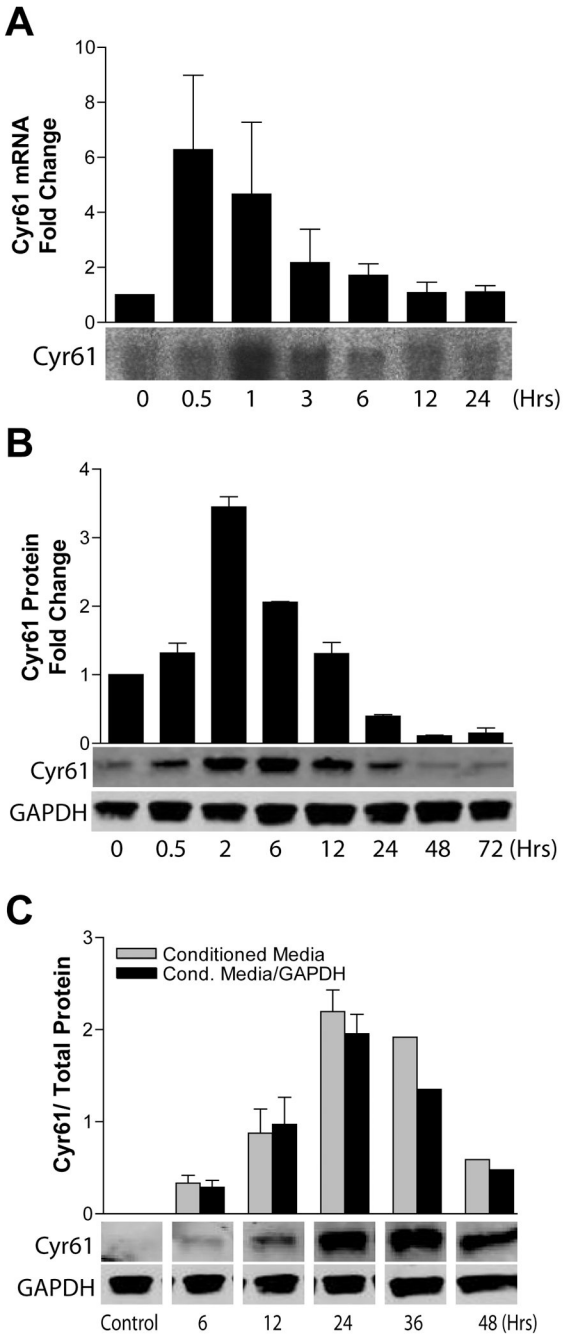

Figure 2. HGF induces Cyr61 in human glioma cell lines

U373 glioma cells were acclimated to low (0.1%) serum for 24 hrs and then stimulated with HGF (50ng/mL) for up to 24 hours. Northern blot analysis (A) and Western blot analysis (B) of whole cell Cyr61 mRNA and protein, respectively, are shown. (C) Cyr61 expression in conditioned medium was concentrated using ultracentrifugation, quantified by immunoblot analysis, and expressed relative to cell layer GAPDH expression. Values expressed are relative to respective controls.

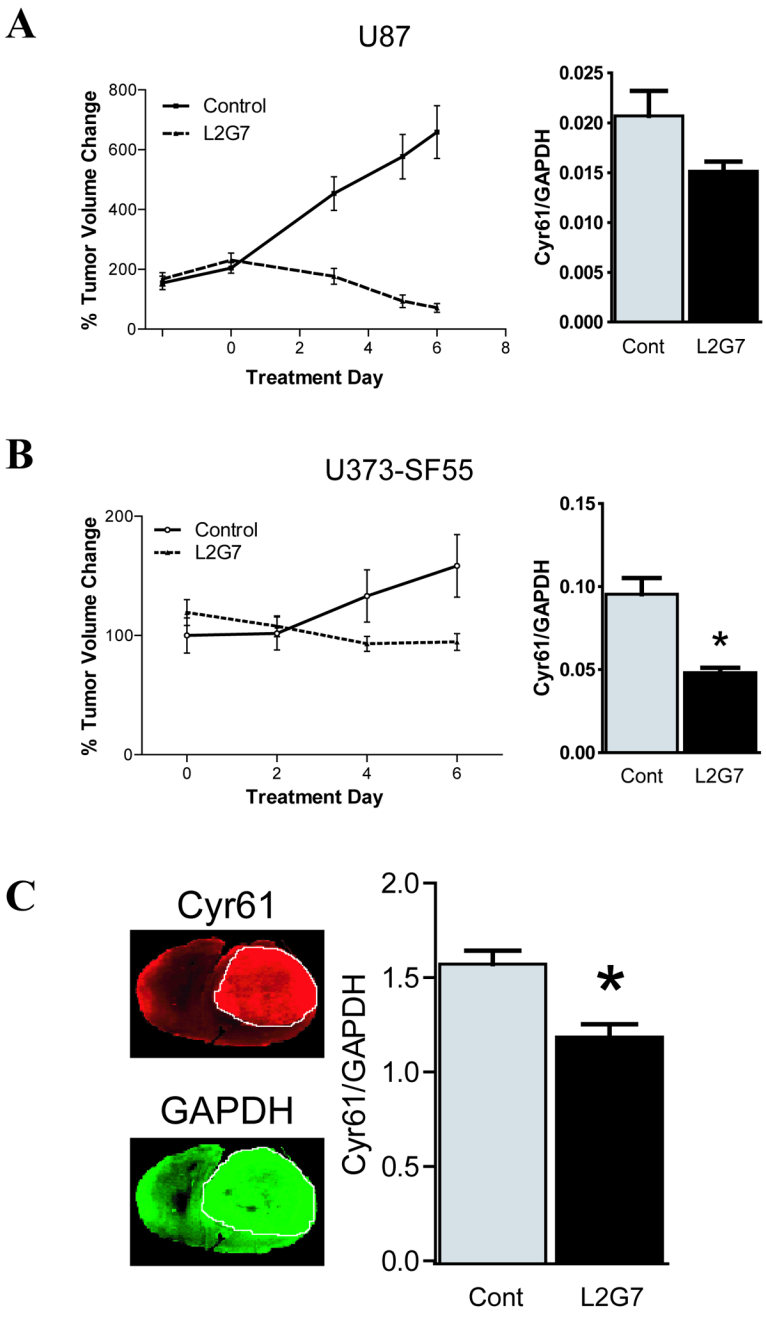

Figure 3. Anti-HGF therapy inhibits Cyr61 expression in vivo

(A) U87 and (B) U373-SF55 HGF-expressing subcutaneous glioma xenografts treated with either control IgG 5G8 or anti-HGF L2G7 (5mg/kg, i.p. every alternate day for a total of three injections) were assessed for tumor volume. Cyr61/GAPDH protein levels were assessed by immunoblot analysis 24 hours after the third injection. (C) Pre-established intracranial U87 glioma xenografts treated as above and analyzed via quantitative dual wavelength infrared immunofluorescent mapping of Cyr61 (red pseudocolor) and GAPDH (green pseudocolor). A representative histological section (left) and the quantification (right) of Cyr61/GAPDH. n = 5 for all groups. Data represents mean ± SEM. * $P < 0.05$ compared to controls.

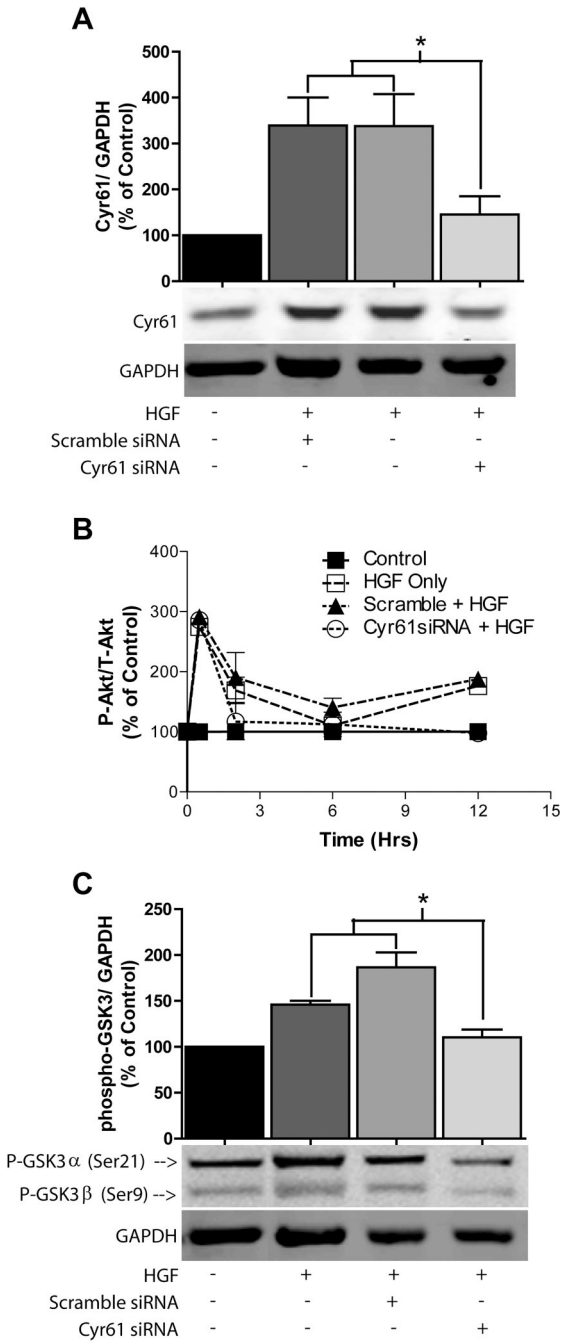

Figure 4. Cyr61 expression knockdown inhibits Akt activation

U373 cells treated with control or Cyr61 siRNA +/− HGF (50ng/mL). (A) Cyr61/GAPDH at 2 Hours post HGF stimulation. (B) Time course of HGF-induced Akt activation in the presence of Cyr61 siRNAs demonstrates p-Akt inhibition at both 2 and 12 hours post HGF-induction ($P<0.05$ compared to scrambled + HGF). (C) Immunoblot analysis of phospho-GSK3 24 hrs after cell stimulation with HGF. * $P < 0.05$ compared to controls.

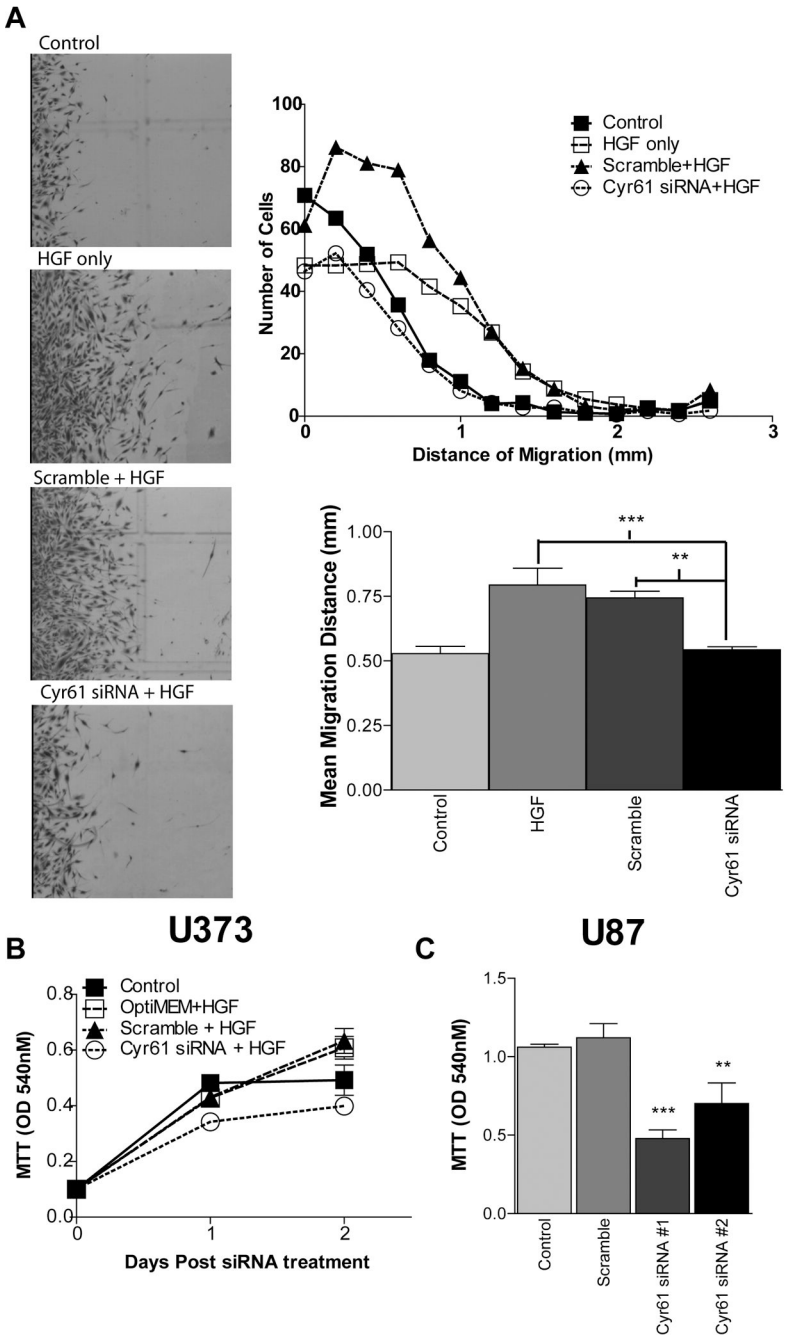

Figure 5. Cyr61 expression knockdown inhibits HGF-induced migration and cell proliferation

(A) Cell migration of growth arrested U373 cells treated with Cyr61 siRNAs (50nM) and stimulated with HGF (50ng/mL) for 6 days. Growth of U373 (B) and U87 (C) cells treated +/− Cyr61 siRNAs 48 hrs following HGF stimulation. ** $P < 0.01$, *** $P < 0.001$ compared to controls.

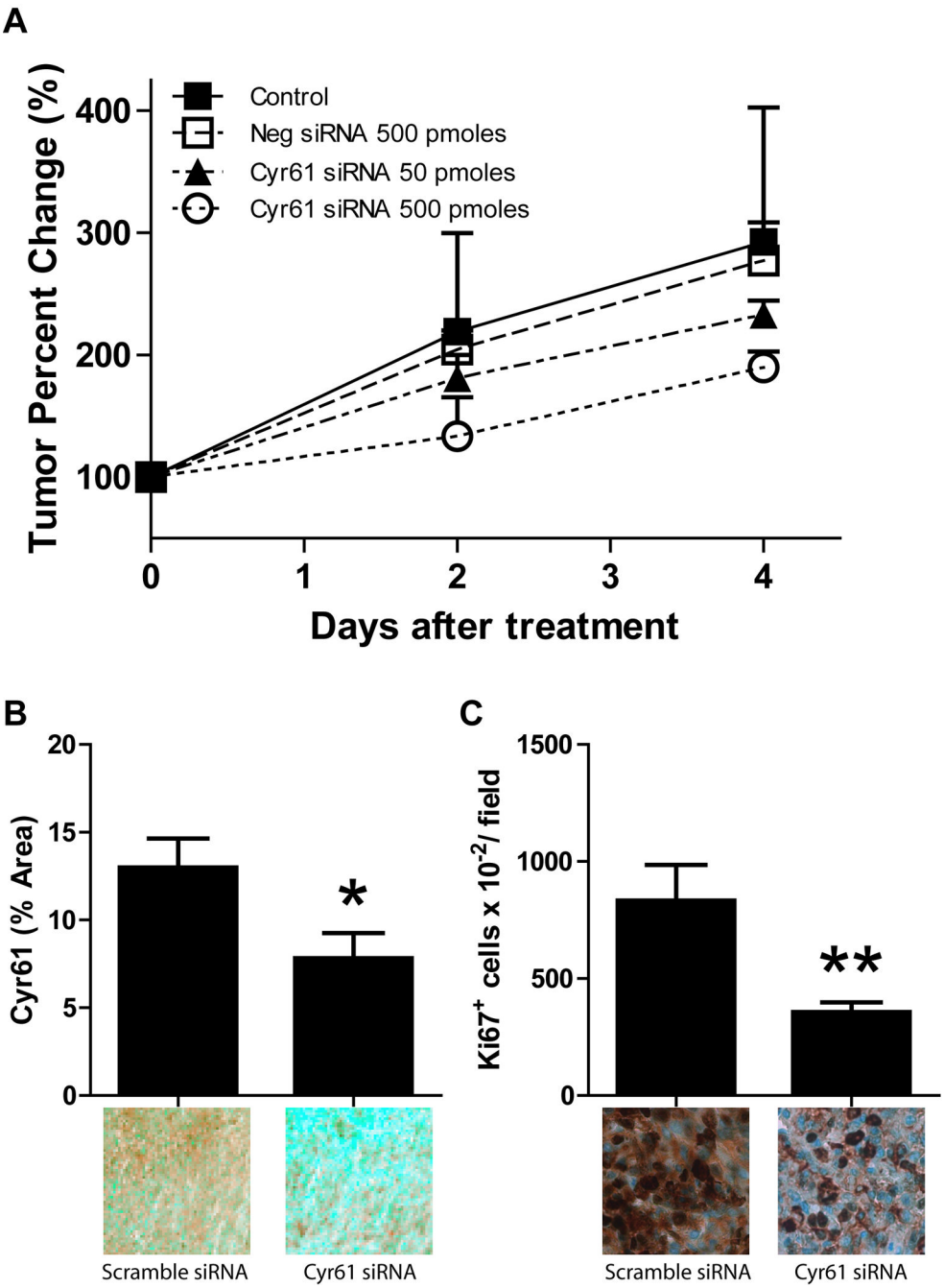

Figure 6. Intratumoral delivery of Cyr61 siRNA inhibits glioma growth in vivo

Pre-established subcutaneous U87 glioma xenografts (treatment started at ~200mm^3) received 50 pmoles or 500 pmoles of Cyr61 siRNA complexed to JET-PEI *in vivo* transfection reagent by intratumoral injection every day for 5 days. All mice were sacrificed 24 hours after the last intratumoral injection. (A) Cyr61 siRNAs (500 pmoles) significantly inhibited U87 glioma xenograft growth by ~35% compared to animals treated with control siRNA ($P < 0.05$). Tissue from tumors treated with control or Cyr61 siRNAs (500 pmoles) were analyzed for Cyr61 expression (B) and tumor cell proliferation (Ki67) (C) by semi-quantitative immunohistochemistry as described in Materials and Methods. Data represents mean ± SEM, n =4 for all groups. * $P < 0.05$, ** $P < 0.001$ compared to controls.